



Evaluation of normal-appearing white matter with perfusion and diffusion MRI in patients with treated glioblastoma

Sinan Şahin¹ · Ersen Ertekin¹ · Tuna Şahin¹ · Yelda Özsunar¹

Received: 1 July 2021 / Revised: 10 December 2021 / Accepted: 12 December 2021 / Published online: 24 December 2021
© The Author(s), under exclusive licence to European Society for Magnetic Resonance in Medicine and Biology (ESMRMB) 2021

Abstract

Objective We tried to reveal how the normal appearing white matter (NAWM) was affected in patients with glioblastoma treated with chemo-radiotherapy (CRT) in the period following the treatment, by multiparametric MRI.

Materials and methods 43 multiparametric MRI examinations of 17 patients with glioblastoma treated with CRT were examined. A total of six different series or maps were analyzed in the examinations: Apparent Diffusion Coefficient (ADC) and Fractional Anisotropy (FA) maps, Gradient Echo (GRE) sequence, Dynamic susceptibility contrast (DSC) and Arterial spin labeling (ASL) perfusion sequences. Each sequence in each examination was examined in detail with 14 Region of Interest (ROI) measurements. The obtained values were proportioned to the contralateral NAWM values and the results were recorded as normalized values. Time dependent changes of normalized values were statistically analyzed.

Results The most prominent changes in follow-up imaging occurred in the perilesional region. In perilesional NAWM, we found a decrease in normalized FA (nFA), rCBV (nrCBV), rCBF (nrCBF), ASL (nASL) values ($p < 0.005$) in the first 3 months after treatment, followed by a plateau and an increase approaching pretreatment values, although it did not reach. Similar but milder findings were present in other NAWM areas. In perilesional NAWM, nrCBV values were found to be positively high correlated with nrCBF and nASL, and negatively high correlated with nADC values (r : 0.963, 0.736, -0.973 , respectively). We also found high correlations between the mean values of nrCBV, nrCBF, nASL in other NAWM areas (r : 0.891, 0.864, respectively).

Discussion We showed that both DSC and ASL perfusion values decreased correlatively in the first 3 months and showed a plateau after 1 year in patients with glioblastoma treated with CRT, unlike the literature. Although it was not as evident as perfusion MRI, it was observed that the ADC values also showed a plateau pattern following the increase in the first 3 months. Further studies are needed to explain late pathophysiological changes. Because of the high correlation, our results support ASL perfusion instead of contrast enhanced perfusion methods.

Keywords Glioblastoma · Radiotherapy · Diffusion MRI · DSC perfusion MRI · ASL perfusion MRI

Introduction

Chemo-radiotherapy (CRT) is a widely used treatment modality for patients with primary or metastatic brain tumors. The standard treatment protocol of glioblastoma includes the use of radiotherapy (RT) with temozolomide chemotherapy for the first month. The aim of RT planning is to minimize the possibility of complications in normal tissues and to ensure tumor cell death at the highest level.

Although advances allow for more precise identification of treated areas, large amounts of healthy tissue are inevitably exposed to significant doses of radiation [1, 2]. Radiation-induced changes in brain tissue can be divided into acute effects, early delayed effects, and late effects [3–6]. Even if late radiation damage is irreversible, understanding its development and quantifying the damage is still unclear [7, 8]. It is known that RT disrupts tissue perfusion by causing vascular damage. It is manifested by dilatation and wall thickening in the vessels, endothelial cell damage, and disruption of the blood–brain barrier in normal-appearing brain tissue [3, 5, 6, 9]. Studies evaluating radiation damage show that white matter is more sensitive than gray matter [10, 11]. Magnetic Resonance Imaging (MRI) is the most effective

✉ Ersen Ertekin
dersen@hotmail.com

¹ Department of Radiology, Adnan Menderes University, Aydın, Turkey

method for imaging brain damage caused by radiation. However, pathological signal changes observed in conventional sequences (T2W series) are not specific and can be seen in processes such as edema, demyelination, and necrosis. In addition, central nervous system damage can be found in areas that appear normal on MRI after RT [8, 12]. For this reason, advanced MRI techniques such as Perfusion MRI and Diffusion Weighted MRI have become frequently used.

There are not many studies evaluating the changes in normal-appearing brain tissue after fractionated radiotherapy (FRT) or stereotactic radiosurgery with perfusion MRI [13–24]. Although there are incompatible findings in these studies, both cerebral blood volume (CBV) and cerebral blood flow (CBF) decreases have been shown in general after FRT or single-fraction stereotactic radiosurgery. Although CBV and CBF data can be calculated with Dynamic Susceptibility Contrast (DSC) MRI, which is widely used in the clinic, it has limitations such as reproducibility and quantification of data acquisition and post-processing [25–31]. Another important method used to evaluate CBF is arterial spin labeling (ASL). There are some studies examining RT-related changes with ASL perfusion [14, 17, 32, 33]. They are advantageous over contrast-enhanced perfusion imaging because they do not require contrast material and are easily reproducible.

Diffusion-Weighted Imaging (DWI) is important in defining the response to RT [34–37] and normal tissue involvement [38–40]. Quantitative Diffusion Tensor Imaging (DTI) measurements are the most sensitive method for identifying white matter abnormalities [41] and vary before any other imaging modality [39, 40]. Generally, DTI changes are progressive and occur after some threshold or in a dose-sensitive manner [40, 42, 43].

In this study, we wanted to evaluate the treatment-related changes over time in normal-appearing white matter (NAWM) with multiparametric MRI in patients with glioblastoma treated with CRT. For this purpose, we analyzed the images of patients who underwent perfusion examination in addition to standard MRI protocols in follow-up imaging. We aimed to evaluate the changes in MRI parameters such as DSC perfusion, ASL perfusion, GRE, DWI, and FA over time and their relationships with each other.

Methods

This retrospective study was approved by the local ethics committee of our institution.

298 patients who underwent MRI between January 2011 and December 2019 were found to have intracranial masses were scanned. Of these patients, 69 patients with unsatisfactory image quality, 17 patients under the age of 18, 160 patients with a diagnosis of non-glioblastoma (78

had benign, 29 had metastasis, and 53 had non-glioblastoma diagnosis), and 35 patients with missing any of MRI sequences on follow-up imaging were excluded from the study. MRI images of 17 patients with pathologically confirmed diagnosis of glioblastoma and treated with the standard CRT regimen were evaluated.

Surgical resection was performed in all patients. Following the healing of the wound, almost 60 Gy was administered in 30 fractions, together with 4–6 weeks of adjuvant chemotherapy, 5 days a week. No patient using chemotherapeutics other than TMZ or receiving RT with a protocol other than the standard treatment protocol before imaging was present in our study.

MRI investigation

MRI investigations were performed using the 1.5 T MR device (Philips Achieva, Philips Medical Systems Nederland B.V.). In addition, tumor perfusion protocol was used in at least one cranial MRI during follow-up in all patients. Initially, conventional cranial MRI, diffusion MRI, and ASL perfusion MRI were performed, respectively without administering any contrast medium. In conventional cranial MRI investigation, axial T1 and T2 weighted (W) sequences, axial FLAIR sequence, sagittal T2W, and axial gradient echo sequences were obtained. Diffusion weighted gradient code was applied in seven directions with a diffusion weight factor of $b = 1000 \text{ s/mm}^2$ for each axial section, and a set of blank images with $b = 0 \text{ s/mm}^2$ was obtained. ADC and FA maps were created from the diffusion tensor.

For perfusion MRI, single-phase ASL involving the entire supratentorial region was obtained without administering any contrast material. The Pulsed ASL (PASL) labeling method available in our system was used. Using single saturation pulses, the post-labeling delay was set to 300 ms and bolus duration was set to 600 ms. Then, DSC perfusion images were obtained with a bolus contrast injection (0.1 mmol/kg) using an automated syringe. For DSC perfusion mapping, the arterial input function (AIF) was defined in the middle cerebral artery, and its proximity, as suggested by Scholdei et al. [44]. Contrast plateaus were marked on the obtained signal intensity-time curves depending on changing sensitivity with the contrast material passing through the cerebral tissues. Then, colour maps (CBV, CBF, and MTT) were created.

The patients' non-contrast and contrast enhanced conventional cranial MRI images, ASL and DSC perfusion images were evaluated via (Picture Archiving Communication Systems) PACS.

Imaging analysis

Two radiologists with 4 and 20 years of experience performed all assessments by consensus. Firstly, T2, FLAIR, and contrast-enhanced images were evaluated, and areas of probable tumor spread, compression, edema effect, and radiation necrosis were excluded.

The areas with no signal alteration, not enhanced after contrast-enhanced imaging in T2W, and FLAIR series were defined as the normal appearing white matter (NAWM). Measurements were made in 14 areas of NAWM in total, seven of which were bilateral in the patient's last investigation included in the study. These areas were as follows:

- 1–2: perilesional ipsilateral-contralateral.
- 3–4: frontal lobe ipsilateral-contralateral.
- 5–6: parietal lobe ipsilateral-contralateral.
- 7–8: occipital lobe ipsilateral-contralateral.
- 9–10: corona radiata ipsilateral-contralateral.
- 11–12: anterior limb of the internal capsule ipsilateral-contralateral.
- 13–14: posterior limb of the internal capsule ipsilateral-contralateral.

Bilateral measurements were made at the same level and similar dimensions (± 3 voxel), creating circular ROIs. Care was taken to keep the standard deviation at a minimum. In follow-up investigations, an effort was made to maintain a similar positioning of ROIs. Initially, the areas were defined in conventional T2w or FLAIR images on PACS, the ROIs were transferred to the FA, ADC, GRE, and single-phase ASL maps at the same levels. Then, measurements were made, and mean values were recorded. Since they represented the gray matter, ROI areas with values under the threshold value of FA = 0.2 were recreated, as described by Chapman et al. [45]. Thus, the areas involving other than

the white matter were excluded. Besides, at the Workstation, similar section levels were aligned on the raw images. Measurements were made on a minimum of three similar-sized ROIs drawn, paying attention to positioning, and the highest rCBF and rCBV values were selected (Fig. 1).

The measurements were normalized. The contralateral, same axial level, mirror-symmetrical, and normal-appearing white matter was used as the reference tissue [22, 43]. Thus, the normalized ADC (nADC), FA (nFA), GRE (nGRE), ASL (nASL), and the normalized relative CBV (nrCBV), normalized relative CBF (nrCBF) values were recorded and used in statistical analysis.

The measurements were divided into seven groups regarding month-based time points as the pretreatment values and the posttreatment values of 1–3, 4–6, 7–9, 10–12, 13–18, and > 18 months. In addition, normalized values of ipsilateral NAWMs were recorded for each time point. Except for perilesional NAWM, the values of other NAWM areas were averaged (frontal, parietal, occipital lobe, corona radiata, anterior and posterior limbs of the internal capsule). Consequently, the averages and standard deviations (SD) of two different values ('perilesional' and 'other NAWM' areas) for the time points they belonged to were calculated and recorded.

Statistical analysis

The statistical analysis of the data was made with SPSS (Statistical Package for Social Sciences, version 20.0; SPSS Inc., Chicago, IL, USA) and MedCalc (MedCalc version 18; Ostend, Belgium) software [61].

Student *T*-test was used to compare two time-point groups. Normality tests (Kolmogorov–Smirnov) determined the distributions of continuous variables. Pearson

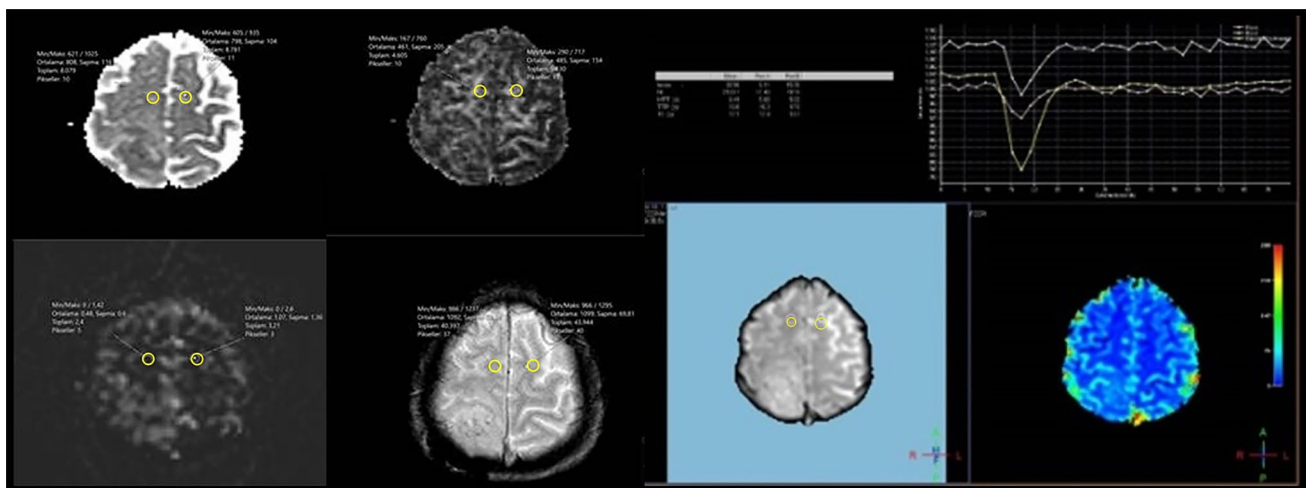


Fig. 1 Placement of sample ROI—Corona Radiata-NAWM- ADC/FA/sfASL/GRE/DSC

Correlation Analysis assessed correlations of changes in different parameters' values over time. The correlation coefficient is expressed by the lowercase 'r,' which is between -1 and $+1$. Values above 0.7 were considered a strong correlation. A p -value < 0.05 was considered statistically significant.

Results

Seventeen patients who met the criteria were included in the study. A total of 43 MRI investigations of 17 patients were evaluated. Among 17 patients, 11 (64.7%) were male, 6 (35.3%) were female, and the mean age was 54.35 (SD: 12.48) years. At the time of data collection, 13 (76.5%) patients died, and treatment and follow-up continued in 4 (23.5%) patients. The mean life duration was 29.3 (SD: 16.67) months in the patients who died. The mass was located in the frontal lobe in seven (41.2%) patients, the parietal lobe in seven (41.2%) patients, and the temporal lobe in three (17.6%) patients. The mean follow-up duration of patients was 13.04 (SD: 11.6) months.

The mean normalized values were recorded after grouping in seven different pre-treatment and post-treatment time points. The values of two different regions were plotted according to their time points, and the significance of changes over time was evaluated. The changes of perilesional mean values and their ' p ' values were presented in Table 1. Figure 2 shows the changes of mean perilesional NAWMs over time.

In perilesional NAWM, even though an almost 20% increase was determined in the 1–3 months group compared to the pre-treatment group, the difference was not statistically significant. This increase was limited to some extent in the 13–18 months and > 18 months groups ($\sim 16\%$), but it was present in all time-point groups at similar rates. In nFA, following RT, a significant reduction of $\sim 19\%$ was

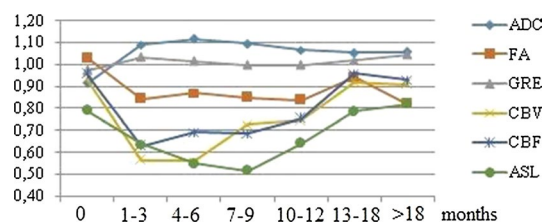


Fig. 2 The changes of mean perilesional NAWM areas over time

determined in the 1–3-month group ($p: 0.0027$), and significant reduction continued in the > 18 months group (20%) ($p: 0.0194$). No significant changes in mean nGRE values with time were determined.

Regarding nrCBV among perfusion values, the mean values of the 1–3 months and 4–6 months time-point groups were $\sim 40\%$ lower than the preRT value ($p: 0.0090$ and $p: 0.0087$, respectively). This value significantly increased in post-RT 10–12 months, 13–18 months, and > 18 months ($p: 0.0300$, $p: 0.0070$, and $p: 0.0069$, respectively), but never returned to its pretreatment levels. Similarly, regarding nrCBF, the mean value of the 1–3 months was ~ 35 lower in the 1–3 months group, $\sim 30\%$ lower in the 4–6 months and 7–9 months groups, compared to its preRT value, and these reductions were statistically significant ($p: 0.0053$, $p: 0.0004$, and $p: 0.0317$, respectively). This value significantly increased in the groups of 13–18 months and > 18 months compared to its value in the 1–3 months group ($p: 0.0002$, and $p: 0.0002$, respectively), but never returned to its pretreatment levels. For nASL, similar to the other perfusion measurements, significant reductions are present in the 1–3 months group ($\sim 20\%$) and the 4–6 months group ($\sim 30\%$) compared to the preRT value ($p: 0.0020$ and $p: 0.0051$, respectively). On the other hand, significant increases were determined in the > 18 months group ($\sim 40\%$, $p: 0.0047$), and values similar to the pretreatment values were reached.

Table 1 The changes of perilesional mean values over time

Perilesional	Pre-treatment	1–3 months	4–6 months	7–9 months	10–12 months	13–18 months	> 18 months
nADC	0.91	1.09	1.12	1.09	1.07	1.05	1.06
nFA	1.03	0.84 ↓ $p: 0.002$	0.87	0.85	0.84	0.94	0.82 ↓ $p: 0.0194$
nGRE	0.97	1.03	1.01	1.00	1.00	1.02	1.05
nrCBV	0.93	0.56 ↓ $p: 0.009$	0.56	0.73	0.74 ↑ $p: 0.03$	0.92 ↑ $p: 0.007$	0.91 ↑ $p: 0.006$
nrCBF	0.96	0.63 ↓ $p: 0.005$	0.69 ↓ $p: 0.004$	0.69 ↓ $p: 0.0317$	0.75	0.96 ↑ $p: 0.0002$	0.93 ↑ $p: 0.0002$
nASL	0.79	0.64 ↓ $p: 0.007$	0.55 ↓ $p: 0.0009$	0.51	0.64	0.78	0.82 ↑* $p: 0.0347$

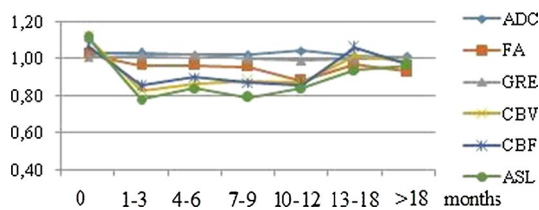
↓ Significant decrease compared to pretreatment period

↑ Significant increase compared to 1–3 months (*compared to 4–6 months) period

Table 2 The correlated perilesional values

Perilesional	nADC	nrCBV	nrCBF	nASL
nADC				
<i>r</i>	1	− 0.973	− 0.908	− 0.809
<i>p</i>		0	0.005	0.028
nrCBV				
<i>r</i>	− 0.973	1	0.963	0.736
<i>p</i>	0		0	0.049
nrCBF				
<i>r</i>	− 0.908	0.963	1	0.716
<i>p</i>	0.005	0		0.041
nASL				
<i>r</i>	− 0.809	0.736	0.716	1
<i>p</i>	0.028	0.049	0.041	

Statistically significant data are indicated in bold

**Fig. 3** The changes in mean values of the other NAWM areas over time

The alterations over time were assessed using Pearson's correlation test. In perilesional NAWM, strong correlations were determined among the mean values of nADC, nrCBV, nrCBF, and nASL. The strongest was the negative correlation between nrCBV and nADC ($r: -0.973$, $p \leq 0.001$). The other strong correlations were nrCBV-nrCBF ($r: 0.963$), nrCBF-nADC ($r: -0.908$), respectively. Moreover, strong correlations of nASL were present with nADC ($r: -0.809$), nrCBV ($r: 0.736$), and nrCBF ($r: 0.716$).

The mean normalized values of ipsilateral frontal, parietal, occipital lobe deep white matter and corona radiata, anterior and posterior limbs of the internal capsule, and the changes of the calculated values over time were presented in Table 2, and the significance of such changes was evaluated. Figure 3 shows the changes in mean values of the other NAWM areas over time.

In the other NAWM areas, no significant changes were determined in nADC and nGRE values over time. In nFA values, when compared to the pretreatment value, a mild but progressive increase was present ($\sim 6\%$ in the 1–3 months time-point group, and $\sim 10\%$ in the > 18 months time-point group); however, the differences were not statistically significant.

The 1–3 months nrCBV values were determined to be significantly reduced ($\sim 25\%$) compared to the preRT values ($p: 0.0178$). In addition, the values were significantly increased in the final time-point group (the > 18 months group) when compared to the posttreatment 1–3 months group ($p: 0.0176$); however, the value did not reach the pretreatment level. Similarly, $\sim 20\%$ significant reduction was determined in the 1–3 months group in nrCBF values ($p: 0.0178$), and a significant increase was observed in the > 18 months group compared to the 1–3 months group ($p: 0.0026$), not reaching the pretreatment values. A similar change was determined in the nASL values; when compared to the pretreatment group, a significant reduction of $\sim 30\%$ ($p: 0.0480$) was determined in the 1–3 months group, $\sim 25\%$ ($p: 0.0020$) in the 4–6 months group, and $\sim 30\%$ ($p: 0.0199$) in the 7–9 months group. Even though $\sim 20\%$ increases were determined in the 13–18 months and > 18 months groups compared to the first posttreatment period ($p: 0.0265$ and $p: 0.0434$), the significant decrease in the > 18 months group compared to the pretreatment period continued ($p: 0.0041$).

The changes of calculated mean values of other NAWM areas in Table 3 over time were evaluated with Pearson's correlation test. Regarding the alterations over time in other NAWM areas, strong correlations of nASL with nrCBV and nrCBF were determined ($r: 0.891$, and $r: 0.864$, respectively). Besides, there was a strong correlation between nrCBV and nrCBF ($r: 0.882$) (Table 4).

Discussion

Our study extended the literature findings that after CRT treatment in patients with glioblastoma, perfusion of white matter areas that appear normal in conventional sequences show a significant decrease and this change is more pronounced than in diffusion sequences. In addition, our study determined that ASL perfusion is at least as sensitive as contrast-enhanced perfusion MRI in showing these changes, in addition to previous studies. The convergence of the defined perfusion and ADC findings with time in follow-up imaging suggests that the damage is partially reversible.

To the best of our knowledge, our study is the first study to evaluate time-dependent changes in NAWM after RT by using PASL and DSC perfusion MRI and DAG parameters such as FA and ADC and to examine the correlation between these methods. We showed significant changes in perfusion measurements in each perfusion method, and a strong correlation between perfusion methods and ADC measurements. In addition, our results make an important contribution to the fact that the ASL perfusion method, which does not require external contrast agent administration, can be used instead of contrast perfusion methods, as the use of contrast

Table 3 The changes in mean values of the other NAWM areas over time

Other NAWM	Pre-treatment	1–3 months	4–6 months	7–9 months	10–12 months	13–18 months	> 18 months
nADC	1.03	1.03	1.02	1.02	1.05	1.01	1.01
nFA	1.03	0.97	0.97	0.96	0.88	0.97	0.93
nGRE	1.01	1.02	1.02	1.00	0.99	1.00	1.01
nrCBV	1.12	0.83 ↓ <i>p</i> : 0.0178	0.87	0.88	0.87	1.02	0.98 ↑ <i>p</i> : 0.0176
nrCBF	1.07	0.86 ↓ <i>p</i> : 0.0178	0.90	0.87	0.86	1.06	0.97 ↑ <i>p</i> : 0.0026
nASL	1.12	0.78 ↓ <i>p</i> : 0.0480	0.84 ↓ <i>p</i> : 0.0020	0.79 ↓ <i>p</i> : 0.0199	0.84	0.94 ↑ <i>p</i> : 0.0265	0.96 ↑* <i>p</i> : 0.0434

Statistically significant data are indicated in bold

↓ Significant decrease compared to pretreatment period

↑ Significant increase compared to 1–3 months (*compared to 4–6 months) period

Table 4 Correlated ‘Other NAWM’ values

Other NAWM	nrCBV	nrCBF	nASL
nrCBV			
<i>r</i>	1	0.882	0.891
<i>p</i>		0.009	0.007
nrCBF			
<i>r</i>	0.882	1	0.864
<i>p</i>	0.009		0.012
nASL			
<i>r</i>	0.891	0.864	1
<i>p</i>	0.007	0.012	

Statistically significant data are indicated in bold

material is increasingly questioned due to its potential side effects.

In this study, we used DSC and PASL perfusion methods to examine vascular damage secondary to CRT, and we found a reduction of up to 40% in nrCBV, 35% in nrCBF, and 30% in nASL in perilesional NAWM with expected high radiation exposure, in 1–3 months and 4–6 months time-point groups. In the other ipsilateral NAWM, we calculated this decrease as approximately 25%, 20%, and 30%, respectively. Our findings show that there is a significant decrease in perfusion over time due to radiation in WM, which does not show any change in conventional MRI series. The decrease in nrCBV, nrCBF, and nASL observed in perilesional and other NAWM areas in the 1-3th month time group, first reach a peak value and draw a plateau in the follow-up images, and then increases, although it does not reach pre-treatment values, after 1 year. This finding indicates that perfusion reduction is largely reversible and transient. Fahlstrom et al. [22] showed a reduction of an average of 5% in nCBV and 4% in nCBF in their study with a shorter follow-up period (3.5 months) using only DSC perfusion MRI, although the use of the overall measurement means

from both hemispheres explains the lesser reduction. Also, similar to our study, they reported a plateau and reversal in the nCBV and nCBF reduction curves, although not statistically significant, after 2 months. In a few similar studies, decreased rCBV and rCBF values returned to pre-treatment or close values in the following periods [18, 20, 23, 24]. All these findings are consistent with the theory that acute and early delayed effects are reversible [3, 5].

In the literature, there are few studies using the ASL perfusion MRI for evaluating the perfusion changes in normal brain tissue after RT, and in these studies, the gray matter was evaluated in general. Petr et al. [17] used the pCASL method in the group of patients older than 18 years of age with a diagnosis of glioblastoma and found a 10% decrease in global CBF values in the contralateral normal appearing gray matter. They reported that similar to our study, the decrease in perfusion varied according to the dose regions (2–16%) and this decrease was stabilized in the late time group. In our study, on the contrary, it was observed that the decrease in perfusion was reversed more significantly, although not reaching pre-treatment values, in later periods, with longer follow-up periods. Similarly, Matthew et al. [45] showed a decrease in perfusion in normal appearing gray matter (NAGM) after RT with the pCASL in patients diagnosed with Medulloblastoma and Pilocytic Astrocytoma, while Taki et al. [15] showed a decrease in NAGM perfusion after RT with gamma rays.

Unlike our study, there are also studies reporting increased perfusion in normal appearing brain tissue after RT, in the literature. Jabukovic et al. [19] reported a 20% increase in rCBV and rCBF values with DSC perfusion MRI, which they evaluated only in the first month. On the other hand, Hu et al. [32] found 9–17% increased perfusion in different regions in the brain tissue that appeared normal in the acute period after RT in patients with nasopharyngeal carcinoma, without distinguishing between gray and white matter. They commented that vasodilatation and increased

blood flow, which occurs as a response of normal brain tissue to radiation in the acute period, can be seen as the cause of increased perfusion.

In this study, we showed that normalized measurements on ADC and FA maps can detect white matter damage and time-dependent changes not seen in conventional series, in NAWM in patients with glioblastoma treated with standard CRT. It is known that RT-induced white matter injury is dose-dependent, and therefore it is inevitable that the WM areas closest to the lesion are more affected [46, 47]. As we move away from the lesion, it is expected that the effect of WM will gradually decrease due to the decrease in the radiation dose exposed. The fact that nADC increase in perilesional NAWM is higher than other NAWM areas in our study supports this information. A similar situation also explains why the decrease in perilesional FA values is higher than in other WM areas. A 20% increase in nADC values and a 19% decrease in nFA values were observed in perilesional NAWM at 1–3 months after RT, indicating loss of axonal integrity in irradiated NAWM areas. A progressive decrease of 10% in mean nFA values in ipsilateral outside of the perilesional (other) NAWM area, although less than in the perilesional area, may suggest the presence of axonal damage. However, we did not detect any significant difference in mean nADC values in other NAWM areas. Similar to our study, Connor et al. [48] using multiple ‘*b*’ values, reported a 10–35% increase in mean diffusivity (MD) and a 7–22% decrease in FA values compared to dose sites. In our study with a longer follow-up period, we found that the increase in ADC values was limited and showed a plateau in the late periods. This finding suggests that disruption of axonal integrity is limited by various injury repair mechanisms. Consistent with this finding, Haris et al. [43] in their study on a limited number of patients reported that the early increase in MD and the decrease in FA detected in high-dose regions were limited in the late periods. In addition, many studies have reported an increase in ADC values and a progressive decrease in FA values in different NAWM areas in patients who received radiotherapy for various reasons [23, 45, 49–52].

In the normalized measurements we performed with T2-FFE, which is a T2-weighted GRE sequence, we did not detect any difference over time both in the perilesional area and in the other ipsilateral NAWM areas. This finding means that there are no significant changes such as calcifications or microbleeds that could cause susceptibility artifacts. There are few studies in the literature evaluating microbleeding after radiation, and most of them used SWI [53–55]. Although SWI is superior in detecting microbleeds [56], in one study using GRE sequences, up to ~26% microbleeding was detected in the white matter later in T2* images [57], and in another study up to 4% reduction in T2* signal has been reported [58]. The reason why no difference

was observed in our study may be due to the GRE imaging parameters we used and the limited number of patients.

There are very few studies evaluating the radiation-related effects of NAWM with both diffusion and perfusion parameters [23, 24, 33]. Nilsen et al. [23] investigated the changes in diffusion and vascular function over time in NAWM after Stereotactic Radiosurgery in patients with brain metastases and evaluated radiation dose regions using DSC Perfusion MRI and diffusion MRI. In their study that included a heterogeneous group with 15–25 GY radiation dose exposure in patients, they found that after reaching the peak value of 5% in the low-dose region and 9% in the high-dose region, it decreased to 2.5% and 3%, respectively. They stated that the reduction in nCBV and nCBF was also partially reversible, similar to ADC. When compared with the reported nCBV and nCBF values, the perfusion improvement that did not return to the pre-treatment values we found in our study is consistent. Naturally, we find more pronounced changes due to the homogeneous patient group and chemotherapy regimen and exposure to a higher amount of standard radiation dose.

In this study, we found a strong correlation between perfusion measurements and nADC measurements in perilesional NAWM exposed to high-dose radiation. The strongest correlation was found between nADC and nrCBV, then between nrCBV and nrCBF. In the other NAWM, a strong correlation was found only between perfusion measurements, and the strongest correlation was between nASL and nrCBV averages. Weber et al. [14] found a strong correlation between the PASL method and DSC perfusion methods, similar to our study, in their study evaluating the contralateral hemisphere with DSC perfusion and two different PASL perfusion methods (ITS-FAIR, Q2TIPS).

In our study, the nASL values, which show a high correlation with the perfusion parameters obtained by the contrast-enhanced DSC MRI method, are remarkable. The use of gadolinium-containing MR contrast agents has become an increasingly questionable subject due to the risk of Nephrogenic Systemic Fibrosis (NSF), which is an accumulation disease that can result in death, restricted use in pregnant women, lactation period and newborns, and possible side effects. For these reasons, the importance of advanced MRI methods without contrast material, such as ASL perfusion, is increasing. In recent years, many studies using the ASL perfusion method have been reported as an alternative to the DSC perfusion imaging method. There are publications reporting that the ASL perfusion imaging is less sensitive to susceptibility artifacts than DSC perfusion [59, 60]. Due to the bolus contrast agent required in DSC perfusion, the advantage of reproducibility in ASL perfusion imaging becomes prominent. Apart from this, providing absolute quantification in ASL-based perfusion examinations and limited exposure due to disruption of the blood–brain barrier

(leaked contrast agent in DSC perfusion examinations causes residual signal loss) are other advantages. For all these reasons and due to the high correlation with contrast-enhanced perfusion MRI in our study, we think that the ASL perfusion method can also be performed for the perfusion studies on the normal appearing brain parenchyma.

Limitations

Due to the retrospective design of the study, the probability of recording errors is high. Although the number of our patients was relatively low, this limitation was attempted by the unity of histopathological diagnosis, homogeneity of the CRT regimen (60 Gy/30 Fr), the lack of use of other known treatment agents, and the high number of analyses. Multivariate analysis was not possible because the number of patients differed between time groups and each patient was not included in each time group. We could not examine dose-dependent changes because the planned dose information before RT could not be included in the examinations. However, we tried to avoid this limitation by grouping perilesional NAWM representing high radiation exposure and ipsilateral other NAWM areas representing average radiation dose exposure. Although circular ROI areas are considered to be a limitation compared to voxel-based measurements, this effect was tried to be avoided by keeping their size (± 3 pixels) similar and the SD value minimal. While selecting the ROI, values less than 0.2, which is suggesting gray matter contamination, in FA measurements were avoided. Another limitation is that it is impossible to differentiate completely from surgical effect and wound healing in the perilesional area. We tried to limit this effect by excluding the enhanced perilesional tissue from the ROI area and evaluating other conventional MR studies such as GRE. In addition, the absence of a significant change in the T2-weighted GRE (T2 FFE) sequence obtained with ROIs in similar areas indicates that areas such as microbleeds that may cause sensitivity artifacts are avoided and that measurements are made from areas that appear normal with conventional series. And finally, ASL perfusion examinations were performed on a 1.5 T MR device using the PASL method, and relatively newer methods such as pCASL with higher Signal-to-Noise-Ratio (SNR) could not be used.

Conclusion

In our current study, we found a perfusion reduction and increased diffusion in NAWM in patients with glioblastoma treated with CRT. We also observed that these findings were more common in the perilesional region due to high radiation exposure. However, we determined that these changes were reversible over time. These findings show that the

brain parenchyma, which appears normal in conventional sequences, is also affected by treatment, and this damage can be demonstrated by perfusion and diffusion MR imaging.

We showed that the power of detecting perfusion changes of the ASL perfusion method is similar to that of the contrast perfusion methods. For this reason, we think that ASL and DCE perfusion methods can be used as biomarkers for the evaluation of CRT-related damage in NAWM, however, ASL perfusion methods should be preferred instead of contrast-enhanced methods due to their high correlation and usage advantages.

Our findings need to be supported by new studies with a larger patient group and standardized follow-up protocol investigating the effects of CRT on normal brain tissue. In addition, studies involving neurocognitive tests and perfusion and diffusion changes in NAWM and the effects of pathophysiological changes on the cognitive status of patients should be evaluated. Thus, the quality of life of the patients can be increased with treatment and post-treatment follow-up arrangements.

Declarations

Conflict of interest The authors declare no conflict of interest.

Ethical statement This retrospective study was approved by the local ethics committee of our institution.

References

- Schultheiss T, Kun L, Ang KK, Stephens L (1995) Radiation response of the central nervous system. *Int J Radiat Oncol Biol Phys* 31(5):1093–1112
- Tofilon PJ, Fike JR (2000) The radio response of the central nervous system: a dynamic process. *Radiat Res* 153(4):357–370
- Kim JH, Jenrow KA, Brown SL (2014) Mechanisms of radiation-induced normal tissue toxicity and implications for future clinical trials. *Radiat Oncol J* 32(3):103–115
- Price RE, Langford LA, Jackson EF, Stephens LC, Tinkey PT, Ang KK (2001) Radiation-induced morphologic changes in the rhesus monkey (*Macaca mulatta*) brain. *J Med Primatol* 30(2):81–87
- Sundgren PC, Cao Y (2009) Brain irradiation: effects on normal brain parenchyma and radiation injury. *Neuroimaging Clin N Am* 19(4):657–668
- Robbins M, Greene-Schloesser D, Peiffer AM, Shaw E, Chan MD, Wheeler KT (2012) Radiation-induced brain injury: a review. *Fron Oncol*. <https://doi.org/10.3389/fonc.2012.00073>
- Shih HA, Loeffler JS, Tarbell NJ (2009) Late effects of CNS radiation therapy. *Cancer Treat Res* 150:23–41
- Kelsey CR, Mukundan S Jr, Wang Z, Hahn CA, Soher BJ, Kirkpatrick JP (2010) Assessing neurotoxicity from the low-dose radiation component of radiosurgery using magnetic resonance spectroscopy. *Neuro Oncol* 12(2):145–152
- Adair JC, Baldwin N, Kornfeld M, Rosenberg GA (1999) Radiation-induced blood–brain barrier damage in astrocytoma:

- relation to elevated gelatinase B and urokinase. *J Neurooncol* 44(3):283–289
10. Tsuruda JS, Kortman KE, Bradley WG, Wheeler DC, Van Dalsem W, Bradley TP (1987) Radiation effects on cerebral white matter: MR evaluation. *Am J Roentgenol* 149(1):165–171
 11. Corn BW, Yousem DM, Scott CB, Rotman M, Asbell SO, Nelson DF, Martin L, Curran WJ Jr (1994) White matter changes are correlated significantly with radiation dose. Observations from a randomized dose-escalation trial for malignant glioma (Radiation Therapy Oncology Group 83–02). *Cancer* 74(10):2828–2835
 12. Crossen JR, Garwood D, Glatstein E, Neuwelt EA (1994) Neurobehavioral sequelae of cranial irradiation in adults: a review of radiation-induced encephalopathy. *J Clin Oncol* 12(3):627–642
 13. Wenz F, Rempp K, Hess T, Debus J, Brix G, Engenhart R, Knopp MV, van Kaick G, Wannenmacher M (1996) Effect of radiation on blood volume in low-grade astrocytomas and normal brain tissue: quantification with dynamic susceptibility contrast MR imaging. *Am J Roentgenol* 166(1):187–193
 14. Weber MA, Günther M, Lichy MP, Delorme S, Bongers A, Thilmann C, Essig M, Zuna I, Schad LR, Debus J, Schlemmer HP (2003) Comparison of arterial spin-labeling techniques and dynamic susceptibility-weighted contrast-enhanced MRI in perfusion imaging of normal brain tissue. *Invest Radiol* 38(11):712–718
 15. Taki S, Higashi K, Oguchi M, Tamamura H, Tsuji S, Ohta K, Tonami H, Yamamoto I, Okamoto K, Iizuka H (2002) Changes in regional cerebral blood flow in irradiated regions and normal brain after stereotactic radiosurgery. *Ann Nucl Med* 16(4):273–277
 16. Price SJ, Jena R, Green HA, Kirkby NF, Lynch AG, Coles CE, Pickard JD, Gillard JH, Burnet NG (2007) Early radiotherapy dose response and lack of hypersensitivity effect in normal brain tissue: a sequential dynamic susceptibility imaging study of cerebral perfusion. *Clin Oncol* 19(8):577–587
 17. Petr J, Platzek I, Seidlitz A, Mutsaerts HJ, Hofheinz F, Schramm G, Maus J, Beuthien-Baumann B, Krause M, van den Hoff J (2016) Early and late effects of radiochemotherapy on cerebral blood flow in glioblastoma patients measured with non-invasive perfusion MRI. *Radiother Oncol* 118(1):24–28
 18. Lee MC, Cha S, Chang SM, Nelson SJ (2005) Dynamic susceptibility contrast perfusion imaging of radiation effects in normal-appearing brain tissue: changes in the first-pass and recirculation phases. *J Magn Reson Imaging* 21(6):683–693
 19. Jakubovic R, Sahgal A, Ruschin M, Pejović-Milić A, Milwid R, Aviv RI (2015) Non tumor perfusion changes following stereotactic radiosurgery to brain metastases. *Technol Cancer Res Treat* 14(4):497–503
 20. Fuss M, Wenz F, Scholdei R, Essig M, Debus J, Knopp MV, Wannenmacher M (2000) Radiation-induced regional cerebral blood volume (rCBV) changes in normal brain and low-grade astrocytomas: quantification and time and dose-dependent occurrence. *Int J Radiat Oncol Biol Phys* 48(1):53–58
 21. Cao Y, Tsien CI, Sundgren PC, Nagesh V, Normolle D, Buchtel H, Junck L, Lawrence TS (2009) Dynamic contrast-enhanced magnetic resonance imaging as a biomarker for prediction of radiation-induced neurocognitive dysfunction. *Clin Cancer Res* 15(5):1747–1754
 22. Fahlström M, Blomquist E, Nyholm T, Larsson EM (2018) Perfusion magnetic resonance imaging changes in normal appearing brain tissue after radiotherapy in glioblastoma patients may confound longitudinal evaluation of treatment response. *Radiol Oncol* 52(2):143–151
 23. Nilsen LB, Digernes I, Grøvik E, Saxhaug C, Latysheva A, Geier O, Breivik B, Sætre DO, Jacobsen KD, Helland Å, Emblem KE (2020) Responses in the diffusivity and vascular function of the irradiated normal brain are seen up until 18 months following SRS of brain metastases. *Neurooncol Adv*. <https://doi.org/10.1093/oaajnl/vdaa028>
 24. Bian Y, Meng L, Peng J, Li J, Wei R, Huo L, Yang H, Wang Y, Fu J, Shen L, Hong J (2019) Effect of radiochemotherapy on the cognitive function and diffusion tensor and perfusion weighted imaging for high-grade gliomas: a prospective study. *Sci Rep* 9(1):1–10
 25. Lacerda S, Law M (2009) Magnetic resonance perfusion and permeability imaging in brain tumors. *Neuroimaging Clin N Am* 19(4):527–557
 26. Jafari-Khouzani K, Emblem KE, Kalpathy-Cramer J, Bjørnerud A, Vangel MG, Gerstner ER, Schmainda KM, Paynabar K, Wu O, Wen PY, Batchelor T, Rosen B, Stufflebeam SM (2015) Repeatability of cerebral perfusion using dynamic susceptibility contrast MRI in glioblastoma patients. *Transl Oncol* 8(3):137–146
 27. Paulson ES, Schmainda KM (2008) Comparison of dynamic susceptibility-weighted contrast-enhanced MR methods: recommendations for measuring relative cerebral blood volume in brain tumors. *Radiology* 249(2):601–613
 28. Petersen E, Zimine I, Ho YL, Golay X (2006) Non-invasive measurement of perfusion: a critical review of arterial spin labelling techniques. *Br J Radiol* 79(944):688–701
 29. Mouridsen K, Christensen S, Gyldensted L, Østergaard L (2006) Automatic selection of arterial input function using cluster analysis. *Magn Reson Med* 55(3):524–531
 30. Knutsson L, Ståhlberg F, Wirestam R (2010) Absolute quantification of perfusion using dynamic susceptibility contrast MRI: pitfalls and possibilities. *MAGMA* 23(1):1–21
 31. Bjørnerud A, Emblem KE (2010) A fully automated method for quantitative cerebral hemodynamic analysis using DSC–MRI. *J Cereb Blood Flow Metab* 30(5):1066–1078
 32. Hu F, Li T, Wang Z, Zhang S, Wang X, Zhou H, Qui S (2017) Use of 3D-ASL and VBM to analyze abnormal changes in brain perfusion and gray areas in nasopharyngeal carcinoma patients undergoing radiotherapy. *Biomed Res* 28(18):7879–7885
 33. Li MD, Forkert ND, Kundu P, Ambler C, Lober RM, Burns TC, Barnes PD, Gibbs IC, Grant GA, Fisher PG, Cheshier SH, Campen CJ, Monje M, Yeom KW (2017) Brain perfusion and diffusion abnormalities in children treated for posterior fossa brain tumors. *J Pediatr* 185:173–180.e3
 34. Thoeny HC, Ross BD (2010) Predicting and monitoring cancer treatment response with diffusion-weighted MRI. *J Magn Reson Imaging* 32(1):2–16
 35. Padhani AR, Liu G, Koh DM, Chenevert TL, Thoeny HC, Takahara T, Dzik-Jurasz A, Ross BD, Van Cauteren M, Collins D, Hammoud DA, Rustin GJ, Taouli B, Choyke PL (2009) Diffusion-weighted magnetic resonance imaging as a cancer biomarker: consensus and recommendations. *Neoplasia* 11(2):102–125
 36. Hamstra DA, Rehemtulla A, Ross BD (2007) Diffusion magnetic resonance imaging: a biomarker for treatment response in oncology. *J Clin Oncol* 25(26):4104–4109
 37. Ellingson BM, Malkin MG, Rand SD, Connelly JM, Quinsey C, LaViolette PS, Bedekar DP, Schmainda KM (2010) Validation of functional diffusion maps (fDMs) as a biomarker for human glioma cellularity. *J Magn Reson Imaging* 31(3):538–548
 38. Uh J, Merchant TE, Li Y, Feng T, Gajjar A, Ogg RJ, Hua C (2013) Differences in brainstem fiber tract response to radiation: a longitudinal diffusion tensor imaging study. *Int J Radiat Oncol Biol Phys* 86(2):292–297
 39. Nazem-Zadeh MR, Chapman CH, Lawrence TL, Tsien CI, Cao Y (2012) Radiation therapy effects on white matter fiber tracts of the limbic circuit. *Med Phys* 39(9):5603–5613
 40. Nagesh V, Tsien CI, Chenevert TL, Ross BD, Lawrence TS, Junick L, Cao Y (2008) Radiation-induced changes in normal-appearing white matter in patients with cerebral tumors: a diffusion tensor imaging study. *Int J Radiat Oncol Biol Phys* 70(4):1002–1010
 41. Bassler PJ, Mattiello J, Le Bihan D (1994) MR diffusion tensor spectroscopy and imaging. *Biophys J* 66(1):259–267

42. Ravn S, Holmberg M, Sørensen P, Frøkjær JB, Carl J (2013) Differences in supratentorial white matter diffusion after radiotherapy—new biomarker of normal brain tissue damage? *Acta Oncol* 52(7):1314–1319
43. Haris M, Kumar S, Raj MK, Das KJ, Sapru S, Behari S, Rathore RK, Narayana PA, Gupta RK (2008) Serial diffusion tensor imaging to characterize radiation-induced changes in normal-appearing white matter following radiotherapy in patients with adult low-grade gliomas. *Radiat Med* 26(3):140–150
44. Scholdei R, Wenz F, Essig M, Fuss M, Knopp M (1999) The simultaneous determination of the arterial input function for dynamic susceptibility-weighted magnetic resonance tomography of the *A. carotis* interna and the *A. cerebri* media. *Rofo* 171(1):38–43 (German)
45. Chapman CH, Nazem-Zadeh M, Lee OE, Schipper MJ, Tsien CI, Lawrence TS, Cao Y (2013) Regional variation in brain white matter diffusion index changes following chemoradiotherapy: a prospective study using tract-based spatial statistics. *PLoS ONE*. <https://doi.org/10.1371/journal.pone.0057768>
46. Zhu T, Chapman CH, Tsien C, Kim M, Spratt DE, Lawrence TS, Cao Y (2016) Effect of the maximum dose on white matter fiber bundles using longitudinal diffusion tensor imaging. *Int J Radiat Oncol Biol Phys* 96(3):696–705
47. Connor M, Karunamuni R, McDonald C, Seibert T, White N, Moiseenko V, Bartsch H, Farid N, Kuperman J, Krishnan A, Dale A, Hattangadi-Gluth JA (2017) Regional susceptibility to dose-dependent white matter damage after brain radiotherapy. *Radiother Oncol* 123(2):209–217
48. Connor M, Karunamuni R, McDonald C, White N, Pettersson N, Moiseenko V, Seibert T, Marshall D, Cervino L, Bartsch H, Kuperman J, Murzin V, Krishnan A, Farid N, Dale A, Hattangadi-Gluth J (2016) Dose-dependent white matter damage after brain radiotherapy. *Radiother Oncol* 121(2):209–216
49. Khong P-L, Kwong DL, Chan GC, Sham JS, Chan F-L, Ooi G-C (2003) Diffusion-tensor imaging for the detection and quantification of treatment-induced white matter injury in children with medulloblastoma: a pilot study. *Am J Neuroradiol* 24(4):734–740
50. Leung LH, Ooi GC, Kwong DL, Chan GC, Cao G, Khong PL (2004) White-matter diffusion anisotropy after chemo-irradiation: a statistical parametric mapping study and histogram analysis. *Neuroimage* 21(1):261–268
51. Qiu D, Leung LH, Kwong DL, Chan GC, Khong PL (2006) Mapping radiation dose distribution on the fractional anisotropy map: applications in the assessment of treatment-induced white matter injury. *Neuroimage* 31(1):109–115
52. Welzel T, Niethammer A, Mende U, Heiland S, Wenz F, Debus J, Krempien R (2008) Diffusion tensor imaging screening of radiation-induced changes in the white matter after prophylactic cranial irradiation of patients with small cell lung cancer: first results of a prospective study. *Am J Neuroradiol* 29(2):379–383
53. Tanino T, Kanasaki Y, Tahara T, Michimoto K, Kodani K, Kakite S, Kaminou T, Watanabe T, Ogawa T (2013) Radiation-induced microbleeds after cranial irradiation: evaluation by phase-sensitive magnetic resonance imaging with 3.0 tesla. *Yonago Acta Med* 56(1):7–12
54. Belliveau J-G, Bauman G, Tay K, Ho D, Menon R (2017) Initial investigation into microbleeds and white matter signal changes following radiotherapy for low-grade and benign brain tumors using ultra-high-field MRI techniques. *Am J Neuroradiol* 38(12):2251–2256
55. Mori N, Miki Y, Kasahara S, Maeda C, Kanagaki M, Urayama S, Sawamoto N, Fukuyama H, Togashi K (2009) Susceptibility-weighted imaging at 3 Tesla delineates the optic radiation. *Invest Radiol* 44(3):140–145
56. Mamlouk MD, Handwerker J, Ospina J, Hasso AN (2013) Neuroimaging findings of the post-treatment effects of radiation and chemotherapy of malignant primary glial neoplasms. *Neuroradiol J* 26(4):396–412
57. Yoo DH, Song SW, Yun TJ, Kim TM, Lee SH, Kim JH, Sohn CH, Park SH, Park CK, Kim IH, Choi SH (2015) MR imaging evaluation of intracerebral hemorrhages and T2 hyperintense white matter lesions appearing after radiation therapy in adult patients with primary brain tumors. *PLoS ONE*. <https://doi.org/10.1371/journal.pone.0136795>
58. Raschke F, Wesemann T, Wahl H, Appold S, Krause M, Linn J, Troost EGC (2019) Reduced diffusion in normal appearing white matter of glioma patients following radio(chemo)therapy. *Radiother Oncol* 140:110–115
59. Deibler A, Pollock J, Kraft R, Tan H, Burdette J, Maldjian JA (2008) Arterial spin-labeling in routine clinical practice, part 3: hyperperfusion patterns. *Am J Neuroradiol* 29(8):1428–1435
60. Detre JA, Zhang W, Roberts DA, Silva AC, Williams DS, Grandis DJ, Koretsky AP, Leigh JS (1994) Tissue specific perfusion imaging using arterial spin labeling. *NMR Biomed* 7(1–2):75–82
61. Med Calc (2020) Statistical Software version 18 (MedCalc Software bv, Ostend, Belgium (R1.10)). <https://www.medcalc.org>. Accessed 22 Sept 2021

Publisher's Note Springer Nature remains neutral with regard to jurisdictional claims in published maps and institutional affiliations.